EFFECT OF THIN FILM TRUNCATION THICKNESS ON THE HEAT TRANSFER UNDERESTIMATION FROM AN EVAPORATING DROPLET ON A PARTIAL WETTING SURFACE

Mehrizi A.A.* and Wang H.
Laboratory of Heat and Mass Transport at Micro-Nano Scale,
College of Engineering, Peking University,
Beijing, 100000
China
E-mail: abbasabouei@yahoo.com, hwang@coe.pku.edu.cn

ABSTRACT

The thin liquid film near the contact line is important for droplet evaporation on a heated surface, however, it remains a challenge for modeling and simulation since it operates from macroscale down to nanoscale. The nanoscale thin film profile has long been unknown; besides in CFD simulations the meshing work for the thin film could be extremely consuming therefore a truncation is needed to disregard the very thin part of the thin film region. The present study is an attempt to simplify the thin film modeling for partially wetting liquids, based on a recent Atomic Force microscope (AFM) experiments that suggested the partially wetting nanoscale thin film are closely following the macroscale profiles. We conduct a theoretical study on an evaporating sessile droplet and evaluate the effect of thin film truncation size on the overall heat transfer. A small spherical droplet with less than 1mm diameter is investigated and the wall superheat is 1 C°. The contact angles are ranged from 5^o to 85^o. We evaluate the effect of the dimensionless truncation ratio, i.e. the ratio of the truncation size and droplet height on the overall heat transfer underestimation. The results show that the dimensionless truncation ratio has a critical effect on the heat transfer calculation while the contact angle and the droplet size have relatively weaker influences. It is due to the fact that the variation of truncation ratio has much more effect on the size of the neglecting thin film region.

Keywords: Droplet, Thin film, Evaporation, Contact angle, Truncation, Heat transfer.

INTRODUCTION

Evaporative thin liquid film near the triple-phase contact line is one of the important phenomenon in different industrial application like thin film coating [1], droplet cooling [2-4], heat exchangers [5] and etc. The heat flux can reach a maximum in the thin film region due to low liquid resistance. This high value flux can be important in small scale applications such as evaporation in heat pipe grooves [3] and small droplet evaporation [6]. Tremendous studies have been done theoretically, numerically [7, 8] and experimentally [9-11] on it. Computational simulation of droplet evaporation as a popular subject has attracted many researchers [7, 12-14]. Heat transfer and hydrodynamic singularities arise at the contact line where the liquid film thickness comes to be extremely thin. For example, Hu and Larson [12] in their finite element simulation for droplet evaporation have found the strong singularity of heat flux near the contact line. They assumed that the heat flux singularity at the droplet edge was of weak consequence of the overall heat transfer and simply ignored it.

The contact line singularity can be avoided by assuming a truncation thickness near the contact line. The thin film with thickness less than the truncation is neglected and the singularity is thus avoided. For example, in Wang et al.'s [15] simulation for meniscus in a millimeter-scale groove, a truncation thickness of 1 micron was assumed. In many simulations the truncation was not explicitly mentioned, but implicitly determined by their meshing setup i.e. the size of the last mesh cell at the contact line [12]. The truncation method greatly facilitates the modeling and simulation but at the same time it causes an underestimation of heat transfer. Due to the low heat transfer resistance, the thin film region along the droplet's perimeter has high heat flux evaporation rate. By considering high heat transfer rate there, when the thin film area is comparable to the total area of the droplet it has great effect on total heat flux. As a result, neglecting the very thin film region cause the heat transfer underestimation. Therefore, it is required to have a smaller truncation thickness to get more accurate results, one needs to put much more effort on the refining mesh in the thin film wedge. The very fine mesh in turn causes great simulation time and computational resources; it could also cause computational errors. In this study, we discuss how to give an acceptable truncation for water droplet evaporation on a partially wetting solid surface.

NOMENCLATURE

g	[m/s^2]	Gravity
h_0	[m]	Droplet height
h	[m]	Height coordinate
h_{fg}	[kj/kg]	Evaporation specific enthalpy
k	[W/mK]	Thermal conductivity
K	[1/m]	Curvature
l	[m]	Capillary length
$\dot{m}''$	[kg/s]	Mass flux
$\bar{M}$	[mol]	Molecular weight
P	[pa]	Pressure
q''	[W/m^2]	Heat flux per area
r	[m]	Radius Coordinate

R	[m]	Contact line radius
$\bar{R}$	[J/mol.K]	Universal gas constant
T	[K]	Temperature

Special characters

θ	[-]	Contact angle
σ	[N/m]	Surface tension
$\hat{\sigma}$	[-]	Interface accommodation coefficient
ϕ	[-]	Dimensionless Temperature $\phi = T_i - T_{sat} / T_s - T_{sat}$

Subscripts

c	Capillary
d	Disjoining
con	Conduction
ev	Evaporation
f	Fluid
i	Interface
Tr	Truncation
v	Vapour
w	Wall

THEORETICAL MODEL

The small sessile water droplet is considered while it is partially wetting the substrate. The surface tension and gravity force play the major role to determine the droplet shape. There is a scale length that shows the transition between the large droplet (considering the gravitational force) and small spherical droplet (neglecting the gravitational force) which is called capillary length $l = \sqrt{\frac{\sigma}{\rho g}}$. The capillary length is of the order of 2 mm for most liquids including water. In this paper the droplet diameter is less than 1 mm so the droplet has the spherical shape (figure 1). We suppose that the droplet do not recede and the evaporation speed is not fast, thus we can approximate it is as stationary droplet with pinned contact line [16].

The height of the spherical cap droplet can be calculated as:

$$h(r) = \sqrt{\frac{R^2}{\sin^2(\theta)} - r^2} - \frac{R}{\tan(\theta)} \quad (1)$$

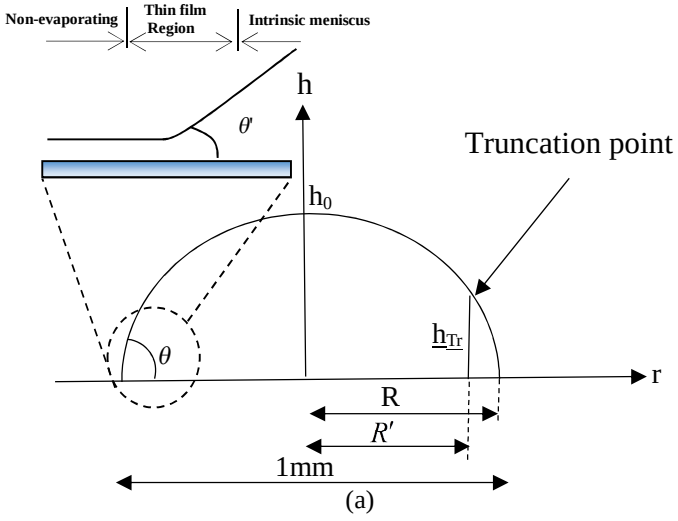

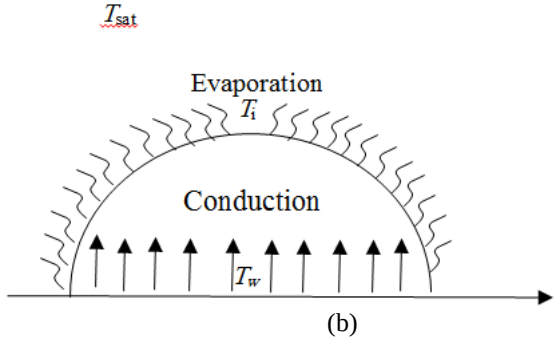

Figure 1 a) the object of this study: a millimeter-scale sessile droplet with spherical cap shape. The macroscopic contact angle θ is approximately equals to the microscopic contact angle θ' based on experimental results [11], h_0 is the maximum height of the droplet and h_{Tr} is the truncation size. b) The heat transfer mechanism during droplet evaporation, the convection and Marangoni flow is neglected [17-19].

Where R is the contact line radius of the droplet (for simplicity we called droplet radious) and θ is the contact angle. According to this assumption that the droplet size is so small, convective flow following the gravity is neglected. Furthermore, by referring to the Girard et al.'s [19] study and this fact that the Marangoni flow was only Strong in highly pure water droplets [17], the Marangoni flow was also neglected. So, the conduction can be considered as the only mechanism that transfers the heat from the substrate through the droplet to the environment (Figure 1 (b)). The conduction heat transfer can be calculated by Fourier's law. So by using a simple one-dimensional conduction equation with linear approximation [20] we will have $q''_{con} = k_f (T_w - T_i)/h$ where k_f is the fluid conductivity, T_w is surface temperature and T_i is the interface temperature. We suppose that the droplet is in the saturated atmosphere and there is no convection there. By applying the energy balance over the interface surface the conduction heat flux should be equal to the evaporation heat flux.

$$q''_{con} = q''_{eva} = q'' \quad (2)$$

The evaporation heat flux over the droplet surface can be calculated by using the evaporative mass flux equation which is derived by using the molecular kinetics-based evaporation theory of Schrage [21]:

$$m'' = \frac{2\hat{\sigma}}{2-\hat{\sigma}} \left(\frac{\bar{M}}{2\pi \bar{R}}\right)^{1/2} \left(\frac{P_{v-eq}(T_i)}{T_i^{1/2}} - \frac{P_v}{T_i^{1/2}}\right) \quad (3)$$

Where $P_{v-eq}(T_i)$ is the equilibrium vapor pressure when there would be no net mass flux across the interface, $\hat{\sigma}$ is the interface accommodation coefficient, $\bar{M}$ is molecular weight and $\bar{R}$ is the universal gas constant. In 1975, Wayner et al. [22] proposed a new model by simplifying the eq. (3) to calculate the mass flux equation which depends on the interface temperature, and the pressure jumps at the interface.

$$m'' = a(T_i - T_v) - b(p_d + p_c) \quad (4)$$

Where

$$a = C\left(\frac{\bar{M}}{2\pi\bar{R}T_i}\right)^{1/2}\frac{P_v\bar{M}h_{fg}}{\bar{R}T_vT_i},\quad b = C\left(\frac{\bar{M}}{2\pi\bar{R}T_i}\right)^{1/2}\frac{V_lP_v}{\bar{R}T_i} \tag{5}$$

In the above equation P_d is disjoining pressure and Pc is capillary pressure and C is the coefficient that equals to $C = 2\hat{\sigma}/2 - \hat{\sigma}$. The disjoining and capillary pressures are:

$$P_c = K\sigma\ ,\ P_d = \frac{A}{6\pi h^3} \tag{6}$$

K is the curvature of the droplet which is equal to $P_c = K\sigma$ $K = \sin(\theta)/R$, σ the surface tension, A the Hamaker constant and h the film thickness. It should be considered that the disjoining pressure only implies under 100 nm film thickness [23, 24].

The heat flux can be calculated as

$$q_{lev}'' = m''h_{fg} \tag{7}$$

The interface temperature and the heat flux can be achieved by solving the Fourier equation, Eq (2) and Eq (7) simultaneously.

In the next step, by selecting different truncations size, we can calculate the amount of heat flux which is underestimated at the certain truncation as follow:

$$q_{tr}'' = \int_{r_c}^{R} q''ds,\quad q_{Total}'' = 2\int_{0}^{R} q''ds \tag{8}$$

Where s is the surface area of the droplet and $ds = 2\pi r dr$. The underestimation heat flux percentage is

$$U = \frac{q_{tr}''}{q_{Total}''}100\% \tag{9}$$

RESULT AND DISCUSSION

A computer code has been developed by using commercial Maple 16 software. The calculation has been done for water droplet with radius between 0.05 mm and 0.5 mm and different contact angle from 5° to 85°. The Hamaker constant for water on SiO2 was calculated to $A = -1\times10^{-20}$ [25]. The surface tension is 7.2×10^{-2} N/m and $\hat{\sigma} = 0.03$. The grid independency test has been performed. The 2 nm, 1 nm and 0.5 nm grid sizes have been investigated and 1 nm size has been found as accurate and economic grid size for all simulations except when the contact angle equals to 5 and 85 and R=0.05 mm, which 0.5nm grid size has been used. To the best of our knowledge, the experimental study that contains all of the criteria in our simulation including the isothermal substarte and saturation environment is rare. To validate our code, we have just selected an experimental study [26] that has better compatibility with our simulation. The droplet was evaporating in a saturated environment, but the substrate temperature was not constant. However, the temperature at the center of the droplet will be constant over time. We have used this temperature as a substrate constant temperature in our simulation. The droplet and environment's details are as follow: The contact angle θ=20° the droplet diameter was 2.3 mm, the saturation temperature was 32°C and the substrate temperature was selected 33.6 °C. According to the experimental result [26] the total evaporation rate was 14.5 µg/s. The total evaporation rate which is calculated by our 1-D simulation was 15.3 µg/s. It has good agreement with experimental result.

The dimensionless temperature $f = (T_i - T_{sat})/(T_s - T_{sat})$ distribution along the droplet surface is presented in figure 2. The result shows that the temperature increases from the top of the droplet to the contact line. For small contact angle the temperature difference is not so considerable, but by augmentation of the contact angle the temperature difference between the contact line and the apex of the droplet increased sharply. Furthermore, at the constant contact angle the temperature difference is increased between the top of the droplet and contact line by enlarging the droplet.

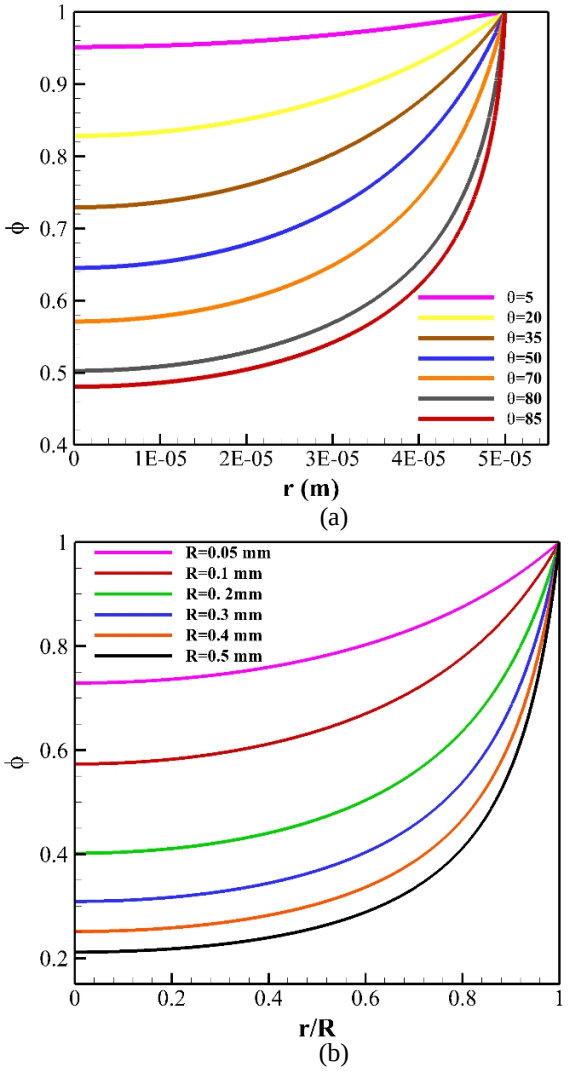

Figure 2 The temperature profile along the droplet surface. a) At different contact angle when R=0.05 mm. b) At different radius when θ=35°.

The heat transfer underestimation versus the dimensionless truncation ratio (h_{Tr}/h_0) when the R=0.3 mm for different contact angle and when θ=35° for different droplet size are presented in Figure 3. The heat flux underestimation percentage for the contact angle between 35° and 65° is close to each other (Figure 3-(a)). When R=0.3 mm, the heat flux

underestimation increased by changing θ from 5° to 50° but by increasing the contact angle from 50° to 85° the underestimation percentage is reduced when the minimum underestimation occurs at θ=85°. It is because of the decreeing the size of the thin film region at very large contact angles. The same trend was observed when the droplet radius is larger than R>0.2 mm. When R is in the range of 0.05 mm to 0.2 mm the heat flux underestimation increased when the contact angle is changed from 5° to θ=35° and then decrease by growing the contact angle to 85. So, the maximum underestimation takes place at θ=35° when R≤0.2 and θ=50° for R>0.2. At R=0.1 the underestimation heat flux for θ=20° and θ=35° is approximately the same (the figure is not presented). It is clear from figure 3-(b) that the truncation size has less effect on smaller droplets for instance, when h_{Tr}/h_0 is equal to 0.1 the underestimation heat flux value change from 10.559% for R=0.05 mm to 19.0% for R=0.5 mm. But, when the dimensionless truncation ratio is so small the effect of the droplet size on heat flux underestimation is not considerable.

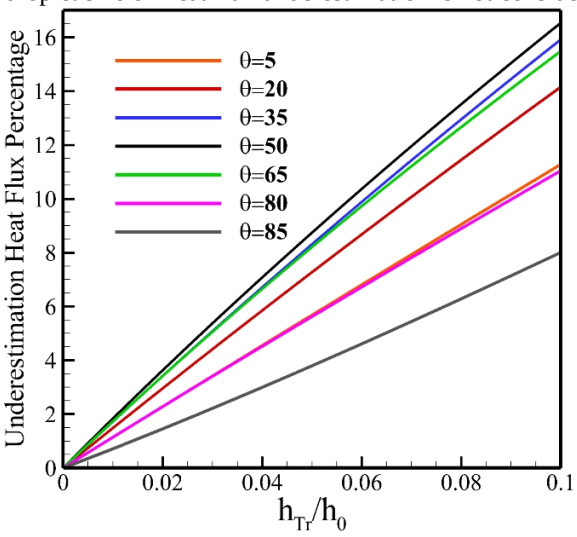

Figure 3 Underestimation heat flux percentage. (a) At different contact angle when R=0.3 mm. (b) At different radius when θ=35°.

Figure 4 shows two heat flux underestimation surfaces for the droplet radius in the range between 0.05 mm and 0.5 mm and the contact angle variation from 5° to 89°. The Truncation size of the lower surface is h_{Tr}=0.25 μm and for the upper surface is h_{Tr}=10 μm. The result shows that h_{Tr}=0.25 μm is acceptable for most of the droplet radius and contact angles except when the droplet size and the contact angle are both small.

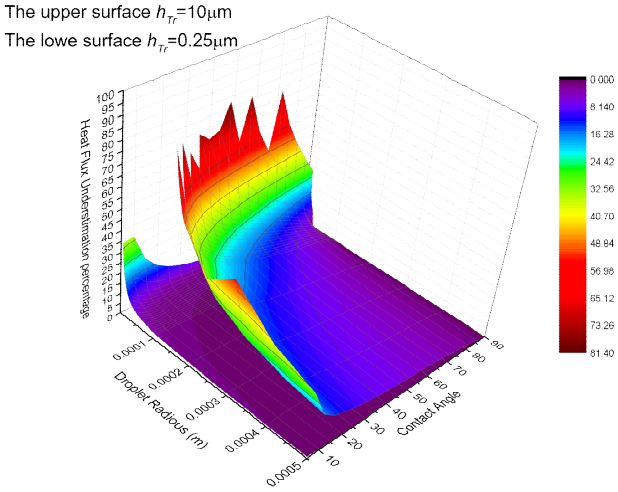

Figure 4 Heat flux underestimation percentage surfaces when h_{Tr}=0.25 μm (the lower surface) and h_{Tr}=10 μm (the upper surface).

We selected two different heat flux underestimation 5% and 10% as an acceptable value for doing the simulation. The optimum truncation size in addition of the dimensionless truncation ratio (h_{Tr}/h_0) for those acceptable heat flux underestimation is presented in Table 1 and Table 2 when the contact angle is 35° and 50°. The contact angle 35° and 50° was selected because the maximum underestimation occurs between these two contact angles. Therefore, the dimensionless truncation ratio is applicable for droplet with other contact angles.

Table 1 The optimum value of truncation size (μm) and dimensionless truncation ratio based on 10% underestimation when θ=35° and θ=50°.

R(mm)	h_{Tr} (μm), θ=35°, (h_{Tr}/h_0)	h_{Tr} (μm), θ=50° (h_{Tr}/h_0)
0.5	7.722, (0.049)	10.506, (0.045)
0.4	6.818, (0.054)	9.407, (0.050)
0.3	5.744, (0.061)	8.0751, (0.058)
0.2	4.414, (0.07)	6.374, (0.068)
0.1	2.652, (0.084)	4.005, (0.086)
0.05	1.493, (0.095)	2.339, (0.10)

Table 2 The optimum value of truncation size (μm) and dimensionless truncation ratio based on 5% underestimation when θ= 35° and θ= 50°.

R(mm)	h_{Tr} (μm), θ=35° , (h_{Tr}/h_0)	h_{Tr} (μm), θ=50°
0.5	3.711, (0.024)	5.0, (0.021)
0.4	3.293, (0.026)	4.502, (0.024)
0.3	2.791, (0.03)	3.895, (0.028)
0.2	2.161, (0.034)	3.107, (0.033)
0.1	1.313, (0.042)	1.982, (0.042)
0.05	0.744, (0.047)	1.170, (0.05)

From the table it is also clear that for R<0.2, the dimensionless truncation ratio at θ=50° is greater than θ=35° and for R≥0.2, the dimensionless truncation ratio at θ=35° is greater than θ=50°. By using Table 1 and Table 2 the researchers can select appropriate truncation size for their computational simulations. For instance, Wang et al.[15] have simulated a millimeter scale evaporative film and they have used 1 μm truncation in their computational simulation. If we select the maximum height of the film as h_0, the dimensionless truncation size for their simulation approximately equals to $h_{Tr}/h_0 \leq 0.001$ and their result has had good agreement with the experimental data.

CONCLUSION

Spherical cap droplet evaporation has been studied theoretically. The effect of truncation size on evaporative heat flux was investigated when the superheat value equals to 1 ℃. The temperature profile along the droplet interface and the heat flux underestimation is presented. The Result showed that the droplet size and the contact angle have great effect on the droplet surface temperature. By increasing the droplet size and droplet contact angle the temperature difference between the top of the droplet and the contact line increased. The heat flux underestimation was also affected by variation of the contact angle and droplet radius, but not as much as the truncation size. The maximum heat flux underestimation occurs when the contact angle changes between θ=35° and θ=50°. The most important factor for heat flux underestimation is the ratio of the truncation size over droplet height. The smallest truncation size and ratio to get 90% and 95% accuracy of total heat flux was calculated and presented. The result showed that to calculate the total heat flux the 0.25 μm truncation size is accurate enough to cover the most range of the droplet size and contact angles.

REFERENCES

[1] Bonn D., Eggers J., Indekeu J., Meunier J. and Rolley E., Wetting and spreading, Reviews of Modern Physics, vol. 81, 2009, pp. 739-805.
[2] Boreyko J.B and Chen C.-H., Self-Propelled Dropwise Condensate on Superhydrophobic Surfaces, Physical review letters, vol. 103, 2009, p. 184501.
[3] Wang H., Garimella, S.V. and Murthy J.Y., Characteristics of an evaporating thin film in a microchannel, Int. J. Heat Mass Transfer vol. 50, 2007, pp. 3933-3942.
[4] Wang H., Garimella S.V and Murthy, J.Y., An analytical solution for the total heat transfer in the thin-film region of an evaporating meniscus, Int. J. Heat Mass Transfer, vol. 51, 2008, pp. 6317-6322.
[5] Panchamgam S.S., Chatterjee A., Plawsky J. L and Wayner Jr,P.C., Comprehensive experimental and theoretical study of fluid flow and heat transfer in a microscopic evaporating meniscus in a miniature heat exchanger, Int J Heat Mass Tran, vol. 51, 2008, pp. 5368-5379.
[6] Karchevsky A.L., Marchuk I.V and Kabov,O.A., Calculation of the heat flux near the liquid–gas–solid contact line, Applied Mathematical Modelling, vol. 40, 2016, pp. 1029-1037.
[7] Barash L.Y., Bigioni T.P., Vinokur V. M and Shchur L.N., Evaporation and fluid dynamics of a sessile drop of capillary size, Phys Rev E, vol. 79, 2009, p. 046301.
[8] Erbil H.Y., McHale G., Rowan S.M., Newton M. I., Analysis of evaporating droplets using ellipsoidal cap geometry, Journal of Adhesion Science and Technology, vol. 13, 1999, pp. 1375-1391.
[9] Yu Y.-S., Wang Z.-Q. and Zhao Y.-P., Experimental study of evaporation of sessile water droplet on PDMS surfaces, Acta Mechanica Sinica, vol. 29, 2013, pp. 799-805.
[10] Cioulachtjian S., Launay S., Boddaert S. and Lallemand, M., Experimental investigation of water drop evaporation under moist air or saturated vapour conditions, International Journal of Thermal Sciences, vol. 49, 2010, pp. 859-866.
[11] Mehrizi A.A. and Wang, H., Nanoscale Thin Film Profile of an Evaporating Water Droplet under Environmental Heating, Int J Heat Mass Tran, vol. On the review, 2016.
[12] Hu H. and Larson R.G., Evaporation of a Sessile Droplet on a Substrate, The Journal of Physical Chemistry B, vol. 106, 2002, pp. 1334-1344.
[13] Hu H. and Larson, R.G., Analysis of the Effects of Marangoni Stresses on the Microflow in an Evaporating Sessile Droplet, Langmuir, vol. 21, 2005, pp. 3972-3980.
[14] Dhavaleswarapu H.K., Murthy J.Y. and Garimella, S.V., Numerical investigation of an evaporating meniscus in a channel, Int J Heat Mass Tran, vol. 55, 2012, pp. 915-924.
[15] Wang H., Pan Z. and Garimella, S.V., Numerical investigation of heat and mass transfer from an evaporating meniscus in a heated open groove, Int J Heat Mass Tran, vol. 54, 2011, pp. 3015-3023.
[16] Cazabat A.M. and Guena G., Evaporation of macroscopic sessile droplets, Soft Matter, vol. 6, 2010, pp. 2591-2612.
[17] Hu H. and Larson, R.G., Marangoni Effect Reverses Coffee-Ring Depositions, The Journal of Physical Chemistry B, vol. 110, 2006, pp. 7090-7094.
[18] Girard F., Antoni M., Faure S. and Steinchen A., Evaporation and Marangoni Driven Convection in Small Heated Water Droplets, Langmuir, vol. 22, 2006, pp. 11085-11091.
[19] Girard F., Antoni, M. and Sefiane K., On the Effect of Marangoni Flow on Evaporation Rates of Heated Water Drops, Langmuir, vol. 24, 2008, pp. 9207-9210.
[20] Di Marzo M. and Evans D.D., 1986, "Evaporation of a water droplet deposited on a hot high thermal conductivity solid surface," National Bureau of Standards.
[21] Schrage R.W., A Theoretical Study of Interface Mass Transfer, Columbia University Press, New York, (1953).
[22] Wayner P.C., Kao Y. and K.LaCroix L.V., The interline heat-transfer coefficient of an evaporating wetting film, Int J Heat Mass Tran, vol. 19, 1976, pp. 487-492.
[23] Ye X., Qu Y. and Li C., Effect of Concentration-dependent Disjoining Pressure on Vertical Draining Flow, Procedia Engineering, vol. 126, 2015, pp. 735-739.
[24] Ajaev V.S., Interfacial fluid mechanics, 2012, Springer.

[25] Butt H.J., Graf K. and Kappl M., 2004, Front Matter, Physics and Chemistry of Interfaces, Wiley-VCH Verlag GmbH & Co. KGaA, pp. i-xii.
[26] Sodtke C., Ajaev V. anf Stephan P., Evaporation of thin liquid droplets on heated surfaces, Heat and mass transfer, vol. 43, 2007, pp. 649-657.